CASE REPORT

Journal of the ASEAN Federation of Endocrine Societies

Phosphaturic Mesenchymal Tumor: From Invisibility to Bedridden Morbidity

Ramita Mukherjee,[1] Santosha Kumar Pattashanee,[1] Brijesh Kumar Singh,[1] Asuri Krishna,[1] Sushant Soren,[1] A Nishikant Damle,[2] M C Sharma,[3] V Seenu[1]

[1]*Department of Surgical Disciplines, All India Institute of Medical Sciences, New Delhi, India*
[2]*Department of Nuclear Medicine, All India Institute of Medical Sciences, New Delhi, India*
[3]*Department of Pathology, All India Institute of Medical Sciences, New Delhi, India*

Abstract

Tumor-induced osteomalacia (TIO) is a rare paraneoplastic syndrome caused by fibroblast growth factor 23 (FGF23) secreting phosphaturic mesenchymal tumors. We report a 53-year-old man with progressive osteomalacia resulting in bedridden status. Renal phosphate wasting despite normal vitamin D, intact parathormone, and renal function raised suspicion of TIO, confirmed by elevated FGF23. However, the occult tumor was localized only by Ga-68 DOTANOC whole-body PET-CT, highlighting the diagnostic challenges in TIO.

Key words: oncogenic osteomalacia, phosphaturic mesenchymal tumor, FGF23, hypophosphatemia, paraneoplastic syndrome

INTRODUCTION

Tumor-induced Osteomalacia (TIO), also known as oncogenic osteomalacia, is a rare paraneoplastic syndrome caused by overproduction of fibroblast growth factor 23 (FGF23).[1] The most common underlying etiology is a phosphaturic mesenchymal tumor (PMT).[2-4]

Biochemically, patients typically present with hypophosphatemia, inappropriately normal or elevated FGF23 levels and low-to-normal circulating 1,25-dihydroxyvitamin D levels. Excess FGF23 reduces renal phosphate reabsorption and suppresses 1-alpha-hydroxylase activity, resulting in impaired bone mineralization. Because TIO is rare and its symptoms are nonspecific, diagnosis is often delayed. Surgical excision is the treatment of choice and is usually curative.[1]

CASE

A 53-year-old male presented with progressively worsening generalized musculoskeletal pain and difficulty rising from a sitting position over two years, eventually resulting in significant functional limitation and a near-bedridden status.

On evaluation, skeletal survey with X-ray (Figure 1A) and MRI pelvis (Figure 1B) demonstrated multiple insufficiency (stress) fractures. Laboratory investigations revealed severe hypophosphatemia, markedly elevated alkaline phosphatase (ALP), and increased 24-hour urinary phosphate excretion, while other biochemical parameters were within normal limits (Table 1). The dual-energy X-ray absorptiometry (DEXA) scan showed severe osteoporosis, likely secondary to chronic hypophosphatemia and defective mineralization.

To determine the etiology of hypophosphatemia, a comprehensive renal tubular evaluation was performed. Urinalysis revealed no glycosuria or proteinuria, and venous blood gas analysis was normal, thereby excluding Fanconi syndrome and proximal renal tubular acidosis (type 2). Further assessment demonstrated renal phosphate wasting, as evidenced by a reduced tubular maximum phosphate reabsorption per glomerular filtration rate (TmP/GFR) of 0.6 mg/dL.

The presence of renal phosphate wasting in the setting of normal serum vitamin D, intact parathyroid hormone (iPTH) and preserved renal function raised strong suspicion for a phosphaturic tumor causing oncogenic osteomalacia. Subsequent measurement of serum FGF23 was markedly elevated at 507 pg/mL (reference range: 23–95 pg/mL), supporting the diagnosis of FGF23-mediated paraneoplastic hypophosphatemia.

eISSN 2308-118x (Online)
Printed in the Philippines

Received: January 16, 2026. Accepted: March 5, 2026.
Published online first: August 13, 2026.
https://doi.org/10.15605/jafes.041.02.5185

Corresponding author: Asst. Prof. Brijesh Kumar Singh, MBBS,MS,MCh
Department of Surgical Disciplines, All India Institute of Medical Sciences,
Ansari Nagar, Sri Aurobindo Marg, New Delhi, India 110029
Tel. No: +91-11-26588500 to700
E-mail: brijeshkumarsinghssmc04@gmail.com
ORCiD: https://orcid.org/0000-0002-9183-2317

Initial clinical examination did not reveal any obvious mass lesion, apart from proximal muscle weakness. This prompted functional imaging to localize the suspected tumor. Ga-68 DOTANOC whole-body PET-CT was performed and demonstrated a somatostatin receptor (SSTR)-expressing subcutaneous soft tissue lesion located lateral to the proximal right fibula, with no evidence of additional SSTR-avid lesions elsewhere in the body (Figure 2).

Following imaging localization, a repeat focused physical examination identified a 3 cm × 3 cm firm, painless, mobile subcutaneous swelling with well-defined margins at the corresponding site (Figure 3). The lesion was clinically inconspicuous and had not been noticed by the patient before.

Selective venous sampling (SVS) was subsequently performed to confirm that the lesion was the source of FGF23 hypersecretion, thereby supporting the PET findings. FGF23 concentration was significantly elevated in the right femoral vein (1870 pg/mL) compared to the left femoral vein (530 pg/mL) and right brachial vein (530 pg/mL), confirming tumor laterality.

A wide local excision with a 1 cm surgical margin was performed under local anesthesia. Postoperatively, serum phosphate levels gradually normalized, accompanied by marked clinical improvement in bone pain and proximal muscle strength. The patient was discharged on postoperative day 10 with calcium and vitamin D supplementation.

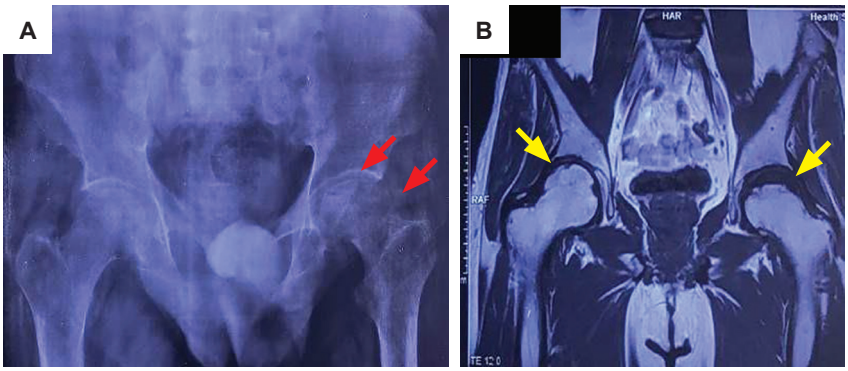

Figure 1. (A) X-ray pelvis showing stress fractures *(red arrows)*. **(B)** MRI Pelvis coronal section showing stress fractures in both femurs. Bilateral femoral head with subchondral fractures and avascular necrosis *(yellow arrows)*.

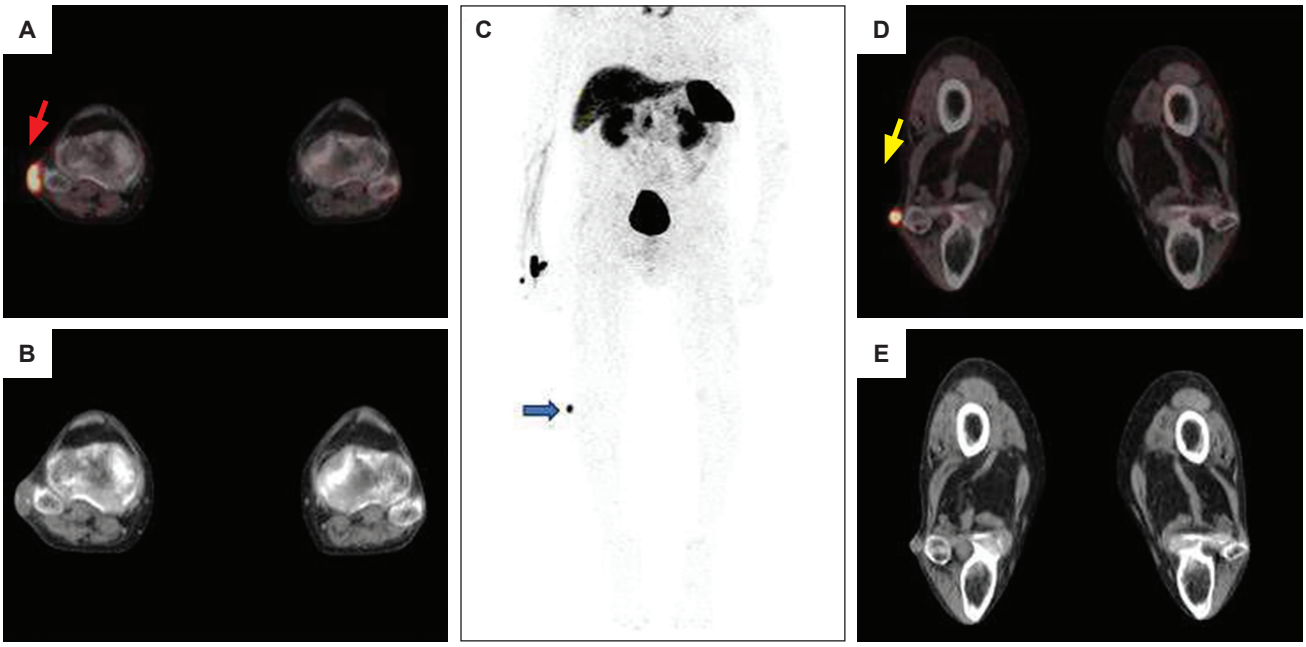

Figure 2. ^{68}Ga-DOTANOC PET/CT localization of the tumor causing tumor-induced osteomalacia (TIO). **(A)** Fused PET/CT images show a focal area of tracer uptake *(red arrow)* in the soft tissue over the lateral aspect of the proximal right fibula, compared with the normal contralateral leg. **(B)** Corresponding CT images of the same region, without PET overlay. **(C)** Whole-body PET image showing normal background tracer uptake (pituitary, liver, spleen, kidneys) and a single abnormal focus in the right leg *(blue arrow)*, corresponding to the tumor. **(D)** Fused PET/CT images at a second level, again showing the tracer-avid lesion *(yellow arrow)*, with the normal leg for comparison. **(E)** CT images *(bone window)* showing a normal, intact fibula, confirming the tumor lies in the soft tissue and does not involve the bone.

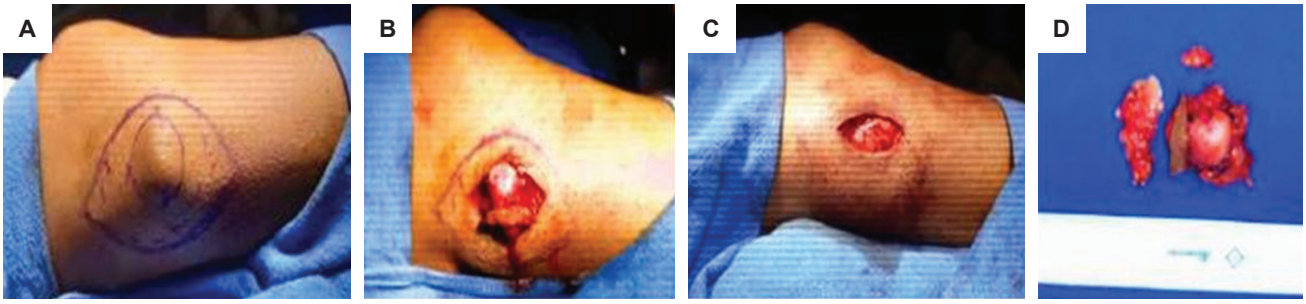

Figure 3. Clinical and intraoperative images of the tumor and resected specimen. **(A)** Preoperative clinical photograph showing the surgical marking outlining the tumor and planned incision over the proximal right leg. **(B)** Intraoperative photograph showing the tumor after incision. **(C)** Intraoperative photograph after tumor excision, showing the resection bed. **(D)** Gross photograph of the resected tumor specimen.

At one-year follow-up, biochemical parameters remained within normal limits, bone mineral density showed improvement, and the patient regained ambulatory function with support. A comparison of pre- and postoperative biochemical parameters and T-scores is presented in Table 1.

Histopathological examination of the excised specimen revealed a circumscribed spindle-cell neoplasm composed of oval to spindle-shaped cells without nuclear atypia, mitotic activity, or necrosis (Figure 4A-C). On immunohistochemistry (IHC), tumor cells were positive for SATB2 and CD56 and negative for CD34, STAT6, and CD99. The findings were consistent with a diagnosis of phosphaturic mesenchymal tumor (PMT) (Figure 4D-F).

Table 1. Biochemical parameters and bone density before and after surgery

Biochemical parameter	Pre-operative	Post-operative			
		Day 0	Day 3	Day 7	1-year
Sodium/ Potassium (mmol/L)	140/4.2				
Urea/ Creatinine (mg/d)	15/0.4				
Calcium (mg/dl)	9.8				
25 (OH) vitamin D (ng/ml)	15.1				
iPTH (pg/ml)	15.1				
Serum phosphate (mg/dl)	0.6	1.9	2.6	3.9	
FGF-23 (pg/ml)	507	55	-	-	
Alkaline phosphatase (U/L)	1171	-	-	-	128
DEXA Scan T-score					
Radius	-6.1	-	-	-	-5.7
Lumbar spine	-5.8				-4.0
Left hip	-3.1				-2.8

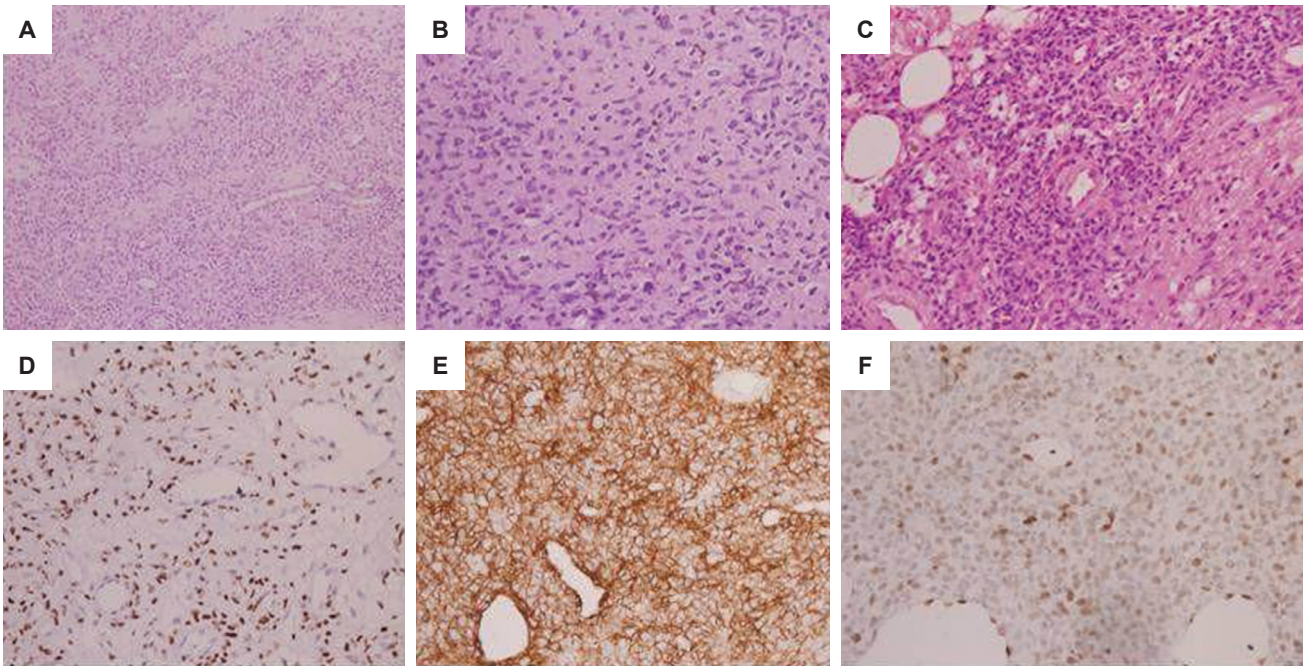

Figure 4. Histopathological and immunohistochemical features of the tumor. **(A–C)** Hematoxylin and eosin (H&E)–stained sections showing a patternless, cellular tumor composed of oval to spindle cells set in an eosinophilic, collagenous stroma with interspersed adipocytes, at increasing magnification. **(D)** Immunohistochemistry showing tumor positivity for ERG. **(E)** Immunohistochemistry showing tumor positivity for CD56. **(F)** Immunohistochemistry showing tumor positivity for SATb2.

DISCUSSION

Tumor-induced osteomalacia (TIO) is a rare paraneoplastic syndrome, with reported incidence and prevalence of approximately 0.13 per 100,000 person-years and 0.70 per 100,000 individuals, respectively.[5] The fundamental biochemical abnormality underlying oncogenic osteomalacia is persistent hypophosphatemia secondary to phosphaturic mesenchymal tumor (PMT)-mediated overproduction of fibroblast growth factor-23 (FGF23).[6]

FGF23 exerts its biological effects by binding to the fibroblast growth factor receptor-1 (FGFR1)–Klotho (KL) receptor complex in the proximal convoluted tubules of the kidney.[7,8] This interaction suppresses the expression of sodium-phosphate cotransporters (NaPi-IIa and NaPi-IIc), resulting in renal phosphate wasting. Concurrently, FGF23 inhibits 1-alpha-hydroxylase activity, thereby reducing the synthesis of 1,25-dihydroxyvitamin D and impairing intestinal absorption of calcium and phosphate.[8] The combination of phosphaturia and impaired mineralization ultimately leads to osteomalacia.

Establishing the diagnosis of TIO requires objective documentation of renal phosphate wasting, typically by calculating the tubular maximum phosphate reabsorption per glomerular filtration rate (TmP/GFR), while excluding generalized proximal tubular dysfunction such as Fanconi syndrome.[9,10] In our patient, TmP/GFR was markedly reduced (0.6 mg/dL). The absence of glycosuria, proteinuria or metabolic acidosis confirms isolated phosphate wasting rather than global tubular dysfunction.

Beyond its systemic effects, FGF23–FGFR1 signalling also contributes to tumorigenesis in PMTs.[11] Approximately 60% of PMTs harbor a fibronectin-1 (FN1)–FGFR1 gene fusion, resulting in constitutive activation of the chimeric FN1-FGFR1 protein driven by strong promoters.[11] Autocrine and paracrine stimulation by tumor-derived FGF23 activates the mitogen-activated protein kinase (MAPK) pathway, promoting cellular proliferation and survival. Additional genetic alterations, including FN1–fibroblast growth factor-1 (FGF1) fusion, have been described in a subset of cases.[12] Although these molecular mechanisms provide insight into tumor biology, clinical recognition remains paramount for timely management.

Phosphaturic mesenchymal tumors are predominantly benign, with malignant transformation and distant metastasis reported rarely.[3,13,14] Histologically, they are composed of spindle to stellate cells derived from inducible skeletal stem cells, embedded within a myxoid or myxochondroid matrix with characteristic "grungy" calcifications and a distinctive intrinsic microvascular pattern. Osteoclast-like giant cells, mature adipocytes and lamellar bone formation may also be present. Tumor cells typically exhibit small nuclei, indistinct nucleoli and low mitotic activity. Immunohistochemically, SATB2 positivity reflects osteoblastic differentiation. Tumors frequently express CD56, SSTR2A, and ERG, while being negative for S100, STAT6, and DOG-1.[15] The histopathological and immunohistochemical features in our patient (Figure 4) were consistent with these established characteristics.

Two large systematic reviews comprising 1979 reported cases have delineated the demographic and clinical profile of TIO.[16,17] Patients commonly experience prolonged diagnostic delay, often exceeding two years, largely due to nonspecific symptoms and the small, clinically occult nature of these tumors. Consistent with these observations, our patient had a symptom duration of more than two years and initially had no clinically detectable mass. Only after functional imaging localization was a small 3 × 3 cm subcutaneous lesion identified on focused re-examination. This underscores the importance of repeated, targeted physical examination guided by imaging findings.

Approximately 80% of TIO cases are attributable to benign PMTs.[16,17] Other reported etiologies include malignant PMT (1.7%), hemangiopericytoma (6.3%), giant cell tumor (1.8%), benign bone tumors (1.6%), bone sarcoma (0.9%), sinonasal hemangiopericytoma-like tumor or glomangiopericytoma (0.8%) and odontogenic tumor (0.8%). Raised FGF23 levels are documented in more than 95% of cases. In our patient, serum FGF23 was markedly elevated (507 pg/mL), and biochemical remission occurred promptly following tumor excision, further confirming the paraneoplastic mechanism.

Surgical resection remains the definitive treatment and is curative in approximately 97% of cases.[18] In our case, wide local excision resulted in normalization of serum phosphate levels, reduction in alkaline phosphatase and significant functional recovery at one-year follow-up, highlighting the reversibility of the metabolic derangement when the source of the excess FGF23 is removed. For unresectable tumors or persistent disease, alternative therapeutic options include radiotherapy, image-guided ablation, somatostatin analogs in OctreoScan-positive tumors and burosumab—a monoclonal antibody that targets FGF23 and prevents its interaction with the FGFR1/Klotho complex.[1,19] In selected cases not associated with elevated FGF23 or those refractory to definitive therapy, oral calcitriol and phosphate supplementation may be considered.[20] Importantly, serum phosphate should be maintained at the lower limit of normal to minimize the risk of secondary and tertiary hyperparathyroidism.[20]

Given that PMTs are frequently small and clinically inapparent, imaging plays a pivotal role in tumor localization. Although somatostatin receptor (SSTR) scintigraphy has been utilized, receptor expression is not entirely specific.[1] 99mTc-hydrazinonicotinamide (99mTc-HYNIC)-octreotide SPECT-CT has demonstrated sensitivity and specificity of 86.3% and 99.1%, respectively.[21] PET-based SSTR imaging modalities—including DOTATATE, DOTANOC, and DOTATOC—are increasingly preferred, with DOTATATE demonstrating higher affinity for SSTR2.[22]

In our patient, Ga-68 DOTANOC PET-CT successfully localized the lesion to the right proximal lower limb (Figure 2). Subsequent selective venous sampling (SVS) demonstrated markedly elevated FGF23 levels in the right femoral vein compared to contralateral and peripheral sites, thereby confirming laterality.[23] Fine-needle aspiration cytology was not performed to avoid potential tumor seeding.[1]

This case reinforces several clinically important principles. In patients presenting with chronic musculoskeletal pain, proximal muscle weakness and stress fractures accompanied by hypophosphatemia with normal calcium, vitamin D and parathyroid hormone levels, a structured and systematic evaluation is essential. Documentation of renal phosphate wasting through TmP/GFR calculation, assessment of FGF23 levels and timely functional imaging are critical steps in diagnosis. Early recognition and definitive surgical management can prevent prolonged morbidity and restore functional capacity, as observed in our patient.

CONCLUSION

Tumor-induced osteomalacia is a rare but treatable cause of severe disability, with phosphaturic mesenchymal tumor being the most common underlying etiology. Early recognition and surgical management can restore function and quality of life. Resection under regional anesthesia, as in our case, helped the patient return to his normal life. An accurate diagnosis is the key to a simple solution for a drastic morbidity.

Ethical Consideration
Patient consent forms were obtained before manuscript submission.

Statement of Authorship
All authors certified fulfillment of ICMJE authorship criteria.

CRediT Author Statement
RM: Conceptualization, Writing – original draft preparation, Investigation; **SKP:** Conceptualization, Writing – original draft preparation, Investigation; **BKS:** Conceptualization, Writing – original draft preparation, Investigation; **AK, SS, AND, MCS:** Conceptualization, Writing – review and editing; **VS:** Conceptualization, Writing – review and editing, Supervision.

Data Availability Statement
No datasets were generated or analyzed for this study.

Author Disclosure
The authors declared no conflict of interest.

Funding Source
None.

References
1. Minisola S, Fukumoto S, Xia W, et al. Tumor-induced osteomalacia: A comprehensive review. Endocr Rev. 2023;44(2):323-53. PMID: 36327295 DOI: 10.1210/endrev/bnac026
2. Folpe AL, Fanburg-Smith JC, Billings SD, et al. Most osteomalacia-associated mesenchymal tumors are a single histopathologic entity: An analysis of 32 cases and a comprehensive review of the literature. Am J Surg Pathol. 2004;28(1):1-30. PMID: 14707860 DOI: 10.1097/00000478-200401000-00001
3. Folpe AL. Phosphaturic mesenchymal tumors: A review and update. Semin Diagn Pathol. 2019;36(4):260-8. PMID: 31301876 DOI: 10.1053/j.semdp.2019.07.002
4. Evans DJ, Azzopardi JG. Distinctive tumours of bone and soft tissue causing acquired vitamin-D-resistant osteomalacia. Lancet. 1972;1(7746):353-4. PMID: 4109739 DOI: 10.1016/s0140-6736(72)92844-9
5. Abrahamsen B, Smith CD, Minisola S. Epidemiology of tumor-induced osteomalacia in Denmark. Calcif Tissue Int. 2021;109(2):147-56. PMID: 33818653 PMCID: PMC8273058 DOI: 10.1007/s00223-021-00843-2
6. Yin Z, Du J, Yu F, Xia W. Tumor-induced osteomalacia. Osteoporos Sarcopenia. 2018;4(4):119-27. PMID: 30775554 PMCID: PMC6372818 DOI: 10.1016/j.afos.2018.12.001
7. Urakawa I, Yamazaki Y, Shimada T, et al. Klotho converts canonical FGF receptor into a specific receptor for FGF23. Nature. 2006;444(7120):770-4. PMID: 17086194 DOI: 10.1038/nature05315
8. Shimada T, Hasegawa H, Yamazaki Y, et al. FGF-23 is a potent regulator of vitamin D metabolism and phosphate homeostasis. J Bone Miner Res. 2004;19(3):429-35. PMID: 15040831 DOI: 10.1359/JBMR.0301264
9. Ackah SA, Imel EA. Approach to hypophosphatemic rickets. J Clin Endocrinol Metab. 2022;108(1):209-20. PMID: 35981346 PMCID: PMC9759174 DOI: 10.1210/clinem/dgac488
10. Hacisahinogullari H, Tekin S, Tanrikulu S, et al. Diagnosis and management of tumor-induced osteomalacia: A single center experience. Endocrine. 2023;82(2):427-34. PMID: 37480497 DOI: 10.1007/s12020-023-03450-3
11. Lee JC, Jeng YM, Su SY, et al. Identification of a novel FN1-FGFR1 genetic fusion as a frequent event in phosphaturic mesenchymal tumour. J Pathol. 2015;235(4):539-45. PMID: 25319834 DOI: 10.1002/path.4465. Erratum in J Pathol. 2015;236(1):131.
12. Lee JC, Su SY, Changou CA, et al. Characterization of FN1-FGFR1 and novel FN1-FGF1 fusion genes in a large series of phosphaturic mesenchymal tumors. Mod Pathol. 2016;29(11):1335-46. PMID: 27443518 PMCID: PMC13417894 DOI: 10.1038/modpathol.2016.137
13. World Health Organization Classification of Tumours Editorial Board. Soft Tissue and Bone Tumours. 5th ed. International Agency for Research on Cancer; 2020
14. Benson JC, Trejo-Lopez JA, Nassiri AM, et al. Phosphaturic mesenchymal tumor. AJNR Am J Neuroradiol. 2022;43(6):817-22. PMID: 35589138 PMCID: PMC9172954 DOI: 10.3174/ajnr.A7513
15. Agaimy A, Michal M, Chiosea S, et al. Phosphaturic mesenchymal tumors: Clinicopathologic, immunohistochemical and molecular analysis of 22 cases expanding their morphologic and immunophenotypic spectrum. Am J Surg Pathol. 2017;41(10):1371-80. PMID: 28614212 DOI: 10.1097/PAS.0000000000000890
16. Álvarez-Rivas N, Lugo-Rodríguez G, Maneiro JR, et al. Tumor-induced osteomalacia: A systematic literature review. Bone Rep. 2024;21:101772. PMID: 38774264 PMCID: PMC11107251 DOI: 10.1016/j.bonr.2024.101772
17. Rendina D, Abate V, Cacace G, et al. Tumor-induced osteomalacia: A systematic review and individual patient's data analysis. J Clin Endocrinol Metab. 2022;107(8):e3428-36. PMID: 35468192 DOI: 10.1210/clinem/dgac253
18. Minisola S, Peacock M, Fukumoto S, et al. Tumour-induced osteomalacia. Nat Rev Dis Primers. 2017;3:17044. PMID: 28703220 DOI: 10.1038/nrdp.2017.44
19. Jan de Beur SM, Miller PD, Weber TJ, et al. Burosumab for the treatment of tumor-induced osteomalacia. J Bone Miner Res. 2021;36(4):627-35. PMID: 33338281 PMCID: PMC8247961 DOI: 10.1002/jbmr.4233
20. Jiang Y, Li X, Huo L, et al; Chinese Society of Osteoporosis and Bone Mineral Research and Chinese Society of Endocrinology. Consensus on clinical management of tumor-induced osteomalacia. Chin Med J (Engl). 2021;134(11):1264-6. PMID: 33813513 PMCID: PMC8183716 DOI: 10.1097/CM9.0000000000001448
21. Shi X, Jing H, Li F, Zhao Y, Wang Z, Huo L. 99mTc-HYNIC-TOC in the evaluation of recurrent tumor-induced osteomalacia. Clin Nucl Med. 2019;44(3):209-13. PMID: 30672760 DOI: 10.1097/RLU.0000000000002458
22. Dahir K, Zanchetta MB, Stanciu I, et al. Diagnosis and management of tumor-induced osteomalacia: Perspectives from clinical experience. J Endocr Soc. 2021;5(9):bvab099. PMID: 34286168 PMCID: PMC8282217 DOI: 10.1210/jendso/bvab099
23. Ito N, Shimizu Y, Suzuki H, et al. Clinical utility of systemic venous sampling of FGF23 for identifying tumours responsible for tumour-induced osteomalacia. J Intern Med. 2010;268(4):390-4. PMID: 20698924 DOI: 10.1111/j.1365-2796.2010.02262.x